Low-frequency ultrasonication modulates the impact of annealing on physicochemical and functional properties of rice flour

Antonio J. Vela; Marina Villanueva; Felicidad Ronda*

Department of Agriculture and Forestry Engineering, Food Technology, College of Agricultural and Forestry Engineering, University of Valladolid, Spain
**Corresponding author. E-mail: fronda@iaf.uva.es*

Abstract

Ultrasonication (US) is a green technology used to physically modify flours to increase their industrial range of applicability. The aim of this work was to study the combined effect that dual US and annealing (ANN) treatments have on starch and protein structure of rice flour, at 20, 40, 50 and 60 °C. Results showed clear modifications of functional, thermal and pasting properties of flours, as well as rheological properties of gels made from them. US+ANN led to generation of small-size particles, which markedly increased the swelling power and starch damage. X-Ray Diffraction and FTIR indicated that starch crystallinity and protein secondary structure was affected by the shear forces of cavitation. The combination of US+ANN improved the crystalline structure arrangement within the starch granules, causing narrowing of the gelatinization temperature range (ΔT). Pasting viscosities were significantly decreased by ultrasonication, following an increasing trend with increasing temperature, while pasting temperature was increased, agreeing in the achievement of a thermodynamically more stable structure. The rheological properties indicated a reduction of the elastic (G') and viscous (G") moduli after ultrasonication, as well as lower values of tan (δ), reflecting a higher predominance of elastic modulus versus viscous one than the non-sonicated flours. The rice flour's properties were found to be highly sensitive to the applied treatment conditions, showing a synergetic effect when sonicating at the highest studied temperature.

Keywords: Rice flour, low-frequency ultrasound treatment, annealing, thermal properties, gel rheological properties; biopolymers structure

1. Introduction

Over the last decade, the market for gluten-free (GF) products has grown considerably. This demand is related to better diagnostic methods identifying an increasing number of people suffering from coeliac disease and other gluten-related disorders, and people who intake GF products as a "healthier" lifestyle (Witczak, Ziobro, Juszczak, & Korus, 2016). As a result, there are increasingly more gluten-free sources studied and transformation techniques applied in the development of novel food products with improved sensorial quality and nutritional value. Flours and starches have been modified by different techniques (genetic, chemical, enzymatic or physical) in order to improve their physical and chemical properties, and increase their industrial range of applicability. Physical modifications are better perceived by consumers for being an environment friendly technology. Physical modification of cereal products by ultrasound (US) treatments have shown many advantages in terms of higher selectivity and quality, reduced use of processing time and chemicals, linked to the concept of "green chemistry and technology", resulting in increasing research interest in recent years (Amini, Razavi, & Mortazavi, 2015; Zhu, 2015).

Physical modifications of flours by US are the result of cavitation phenomenon over the treated matter. Mechanical waves of ultrasonic frequency generate tiny bubbles as result of pressure variation, which keep growing until the oscillation of their walls equals the applied frequency and collapse (Ashokkumar, 2015; Zheng et al., 2013). Collapsing bubbles induce solvent micro-jets shooting to the suspended particles' surface, generating very high shear forces that cause mechanical damage and surface erosion, and local rises of temperature that lead to rise of the suspension's temperature, when the temperature of the treated medium is not controlled (Zhu, 2015). The extent of the modification depends on parameters such as duration, temperature, frequency and power of the treatment, moisture content of the system and botanical origin of the source (Zhu, 2015). Previous studies have demonstrated the great influence that temperature has on the modification achieved on starches (Amini et al., 2015; Kaur & Gill, 2019; Monroy, Rivero, & García, 2018; Sujka & Jamroz, 2013; Zheng et al., 2013).

The rise of temperature in excess water represents a physical modification method called annealing (ANN). The said modification procedure happens when the treated matter is kept in excess water content (>60% w/w) for an extended period of time, at a temperature above the glass transition temperature and below the onset gelatinization temperature, which allows a modest molecular reorganization (Hoover & Vasanthan, 1994; Tester & Debon, 2000; Zavareze, Renato, & Dias, 2011). ANN facilitates interaction between starch chains within the amorphous and crystalline regions,

causing rearrangement to a more organized configuration, which reflects in an improvement of paste viscosity, stability and starch *in vitro* enzymatic digestion (Chi et al., 2019; Zavareze et al., 2011).

The physical modification of starches from different botanical origin has been studied by the individual effect of both US (Amini et al., 2015; Jambrak et al., 2010; Luo et al., 2008; Zuo et al., 2009) and ANN (Chi et al., 2019; Hoover & Vasanthan, 1994; Tester, Debon, & Sommerville, 2000; Wang et al., 2017) treatments and have proven to generate changes in their physical, thermal and hydration properties. In flours, however, very little work is available (Zhu & Li, 2019, Vela et al., 2021). It is important to study both treatments in flours because they are primarily raw materials for starchy food products which are the main source of complex carbohydrates in the human diet. Flours are a more complex matrix than starches and include other components, in particular proteins which are also susceptible to be affected by treatments (Vela et al., 2021). In addition, these components interact with starch in such way that the modification effect on starch is non-comparable to flour.

US treatments, as they must be performed on a water suspension of the sonicated matrix, are commonly joined with ANN treatment, resulting from temperature rise derived from cavitation; so the final characteristics of the treated matter depend on a combined effect of both treatments. However, the individual effect of each treatment is not usually evaluated, and even, not infrequently, the temperature reached in the suspension during treatment is not controlled or monitored at all. The impact of US treatments on rice flour has been previously studied at different concentration and treatment time at a constant treatment temperature of 20° C (Vela, Villanueva, Solaesa, & Ronda, 2021). However, a study of the role that temperature (ANN) plays in the range of modification achieved by ultrasonication has not been covered in the available literature so far. Therefore, the objective of this study was to evaluate the synergistic effect of temperature and ultrasonication on the physical, thermal and hydration properties of rice flour, at the temperatures of 20, 40, 50 and 60 °C. The impact of this dual treatment on flour microstructural arrangement and biopolymers (starch and proteins) structural features was also evaluated.

2. Materials and methods

2.1 Rice flour

The rice flour used was supplied by Emilio Esteban SA (Valladolid, Spain). The composition was: 7.60 % protein, 5.52 % fiber, 2.06 % fat, 0.34 % ash and 13.67 % moisture (data provided by the manufacturer). The native flour was stored at 4 °C until utilization.

2.2 Ultrasound treatment

The equipment used in this study consisted of Hielscher UP400St sonicator (Hielscher Ultrasonics, Germany) set with S24d22D titanium tip. Rice flour dispersions were prepared at a concentration of 10 % (g dry flour/100 g of dispersion) by suspending rice flour in distilled water (total weight of 400 g). All treatments were performed for 60 minutes at constant frequency of 24 kHz with maximum output power of 180 W (47 W/cm^2), and 80 % on-off pulse (0.8 s on 0.2 s off). Treatment time was chosen to be 60 minutes to set it as basis for the annealing treatments. The control flour onset gelatinization temperature was found to be 61.1±0.2 °C, so the treatment temperatures chosen were 20, 40, 50 and 60 °C. Studied samples were sonicated at the constant target temperature, representing a combined US+ANN treatment, and were compared to their corresponding ANN treatment, which were processed following the same procedure without being sonicated (refer to Table 1). The native flour was used without any processing as control in the study. The dispersions were treated in a glass jacket containing recirculating water from a water bath to achieve the desired temperature and maintain it during treatment. During the treatments all dispersions were stirred using a magnetic stirrer to ensure a homogenous temperature and avoid sedimentation of the flour. In ANN treatments the target temperature was directly set in the water bath, while in US+ANN treatments a lower temperature was set in the water bath (10°C below the target temperature) since previous assays had demonstrated that temperature rise derived from ultrasonication would get the dispersions to the desired temperature. Dispersions' temperature was controlled during the whole treatment using a Testo 735-2 (Instrumentos Testo S.A., Spain) digital thermometer coupled with a flexible immersion tip. Flours were retrieved by freeze-drying, using a SP Scientific equipment, model Genesis Pilot Lyophilizer (SP Industries Inc, Warminster, U.S.A.), followed by sieving to <250µm. All treated flours were stored at 4 °C until use.

Table 1. Treatment conditions and sample code given to each flour in the study.

Sample	Ultrasonicated	Temperature (°C)
Control	No	--
ANN-20	No	20
ANN-40	No	40
ANN-50	No	50
ANN-60	No	60
US+ANN-20	Yes	20
US+ANN-40	Yes	40
US+ANN-50	Yes	50
US+ANN-60	Yes	60

2.3 Particle size distribution

The particle size distribution of all flours was determined using a Mastersizer 2000 laser diffraction particle size analyzer (Malvern Instruments Ltd, UK). The reported results are median diameter (D_{50}) and ((D_{90}-D_{10})/D_{50}) as a dispersion measurement, as described in (Abebe, Collar, & Ronda, 2015). Measurements were made in triplicate.

2.4 Scanning electron microscopy (SEM)

Images of the surface microstructure were obtained using a Quanta 200FEG scanning electron microscope (FEI, Oregon, U.S.A.) equipped with X-ray detector, without prior metallization. Visualizations were performed with accelerating voltage of 5.0 keV in low vacuum mode using a secondary electron detector at a magnification of 100x, 500x and 1500x.

2.5 Starch damage

Damaged starch content was measured following the procedure indicated by Vela, Villanueva, Solaesa, & Ronda (2021) using Megazyme starch damage kit (K-SDAM, Megazyme, Ireland). Results are referred to dry matter (dm). Samples were evaluated in triplicate.

2.6 Hydration properties

Water absorption capacity (WAC) was measured at 10% flour dispersion (w/v), while water absorption index (WAI), water solubility index (WSI) and swelling power (SP) were measured at 5% (w/v) following the method described by Abebe, Collar, & Ronda, (2015). All results are referred to flour dry matter. WAC was expressed in g H_2O/g, WAI in g sediment/g, WSI in g soluble solids/100 g and SP in g sediment/g of insoluble solids in flour. Samples were evaluated in triplicate.

2.7 X-Ray diffraction (XRD)

A Bruker-D8-Discover-A25 diffractometer (Bruker AXS, Rheinfelden, Germany) equipped with a Cu-Kα radiation (λ = 0.154 nm) at voltage of 40 kV and current of 40 mA was used to obtain the XRD patterns of the flours. Radiation intensities were measured in the range of 5° to 40° of 2θ diffraction angle, with scan step size of 0.02°, receiving slit width of 0.02nm, scatter slit width of 2.92°, divergence slit width of 1° and a rate of 1.2°/min. Samples were equilibrated at 15% humidity prior measurement using a saturated humidity ICP260 incubator at 15 °C (Memmert GmbH, Germany). Sample's crystallinity was calculated as described in Vela, Villanueva, Solaesa, & Ronda (2020).

2.8 Fourier transform infrared spectroscopy (FTIR)

FT-IR Nicolet iS50 spectrophotometer (Thermo Fisher Scientific, U.S.A.) equipped with a crystal diamond attenuated total reflectance (ATR) sampling accessory was used to record FTIR spectra of the flours, previously equilibrated at 15 % humidity (see section 2.7). Measurements were performed in wavenumber range of 400-4000 cm^{-1} with resolution of 4 cm^{-1} and accumulation of 64 scans. Amide I bands (1700-1600 cm^{-1}) were analyzed using Origin2019b (OriginLab Corporation, U.S.A.). Individual bands were determined in deconvolved curves with second derivative analysis following iterative fitting assuming Gaussian band shapes. Peaks assignment correspond to: β-turns (1700-1660 cm^{-1}), α-helix (1658-1650 cm^{-1}), random coil (1650-1640 cm^{-1}) and β-sheet (1640-1600 cm^{-1}) (Byler & Susi, 1986). Measurements were performed in triplicate.

2.9 Differential scanning calorimetry (DSC)

Flours' thermal properties were determined with DSC3 calorimeter (Mettler Toledo, Spain). A sample of ~6 mg was weighed in 40 μL aluminum pan, and distilled water was added to reach ~30 % w/w flour concentration. The assay was carried out in excess of water, so that there was no limitation to gelatinization. Pans were sealed and kept for 30 min at room temperature prior measurement. Measurements were made from 0 to 110 °C at 5 °C/min heating rate, using an empty sealed pan as reference. Onset (T_O), peak (T_P) and endset (T_E) temperatures (°C) and enthalpy of gelatinization (ΔH) (J/g flour dm) were quantified. A second run of the same procedure was performed after 7 days of sample storage in the pans at 4 ± 2 °C, to study retrogradation transitions. Samples were measured in duplicate.

2.10 Pasting properties

Pasting properties were determined as described by Vela et al. (2021), using a Kinexus Pro+ rheometer (Malvern Instruments Ltd, UK) coupled with starch pasting cell geometry. Each sample (3.50 g on 14% moisture basis) was mixed with 25.0±0.1mL of distilled water in the test canister. Paddle speed was set at 160 rpm. The sample was equilibrated at 50 °C for 1 min, heated to 95 °C at 6 °C/min, maintained at 95 °C for 5 min, then cooled to 50 °C at 6 °C/min, and maintained at 50 °C for 2 min. rSpace software (Malvern Instruments Ltd, UK) was used to calculate pasting temperature (PT), peak viscosity (PV), trough viscosity (TV), breakdown viscosity (BV), final viscosity (FV) and setback viscosity (SV). Samples were measured in duplicate.

2.11 Rheological properties of gels made from studied flours

Dynamic oscillatory tests were performed using Kinexus Pro+ rheometer (Malvern Instruments Ltd, UK) as described by Vela et al. (2021) with serrated parallel plate geometry (40 mm diameter) and a working gap of 1 mm. The gel samples were prepared following the protocol described in section 2.10 for testing the pasting properties and left on the bottom plate to rest for 5 min to allow relaxation. Gels were analyzed by strain sweeps from 0.1 to 1000 % strain at constant frequency of 1Hz, and frequency sweeps from 10 to 1 Hz at 1 % strain, within the linear viscoelastic region (LVR). Data obtained from frequency sweeps were adjusted to the potential equations as described by Ronda, Villanueva, & Collar (2014). Measurements were performed in duplicate.

2.12 Statistical analysis

Results were statistically analyzed using Statgraphics Centurion XVIII software (Bitstream, Cambridge, MN, U.S.A.). Analysis of variance (ANOVA) by Least Significant Difference (LSD) test at p-value ≤ 0.05 was performed.

3. Results and discussion

3.1 Effect of treatment on morphology and particle size distribution

Selected micrographs are presented in Fig. 1. Control flour showed a polygonal arrangement of tightly packed starch granules entwined with globular protein bodies and lipids, characteristic of rice flours (Villanueva, Harasym, Muñoz, & Ronda, 2018). Sonication led to general breakage of said compact structures (US+ANN-20 and US+ANN-60). ANN-20 (which can be seen as processing control for being handled at the lowest temperature) remains with a similar appearance to the control flour in all magnifications. ANN-60, however, presents a more unified structure, losing the visibility of individual starch granules within the arrangement, believed to be consequence of a partial melting caused by treatment temperature (60°C). The 500x and 1500x magnifications of sonicated samples (C2, C3, E2, and E3) reveal more uneven surface, with more exposed and loosen starch granules, in contrast to control and ANN samples that show a flatter and more regular surface.

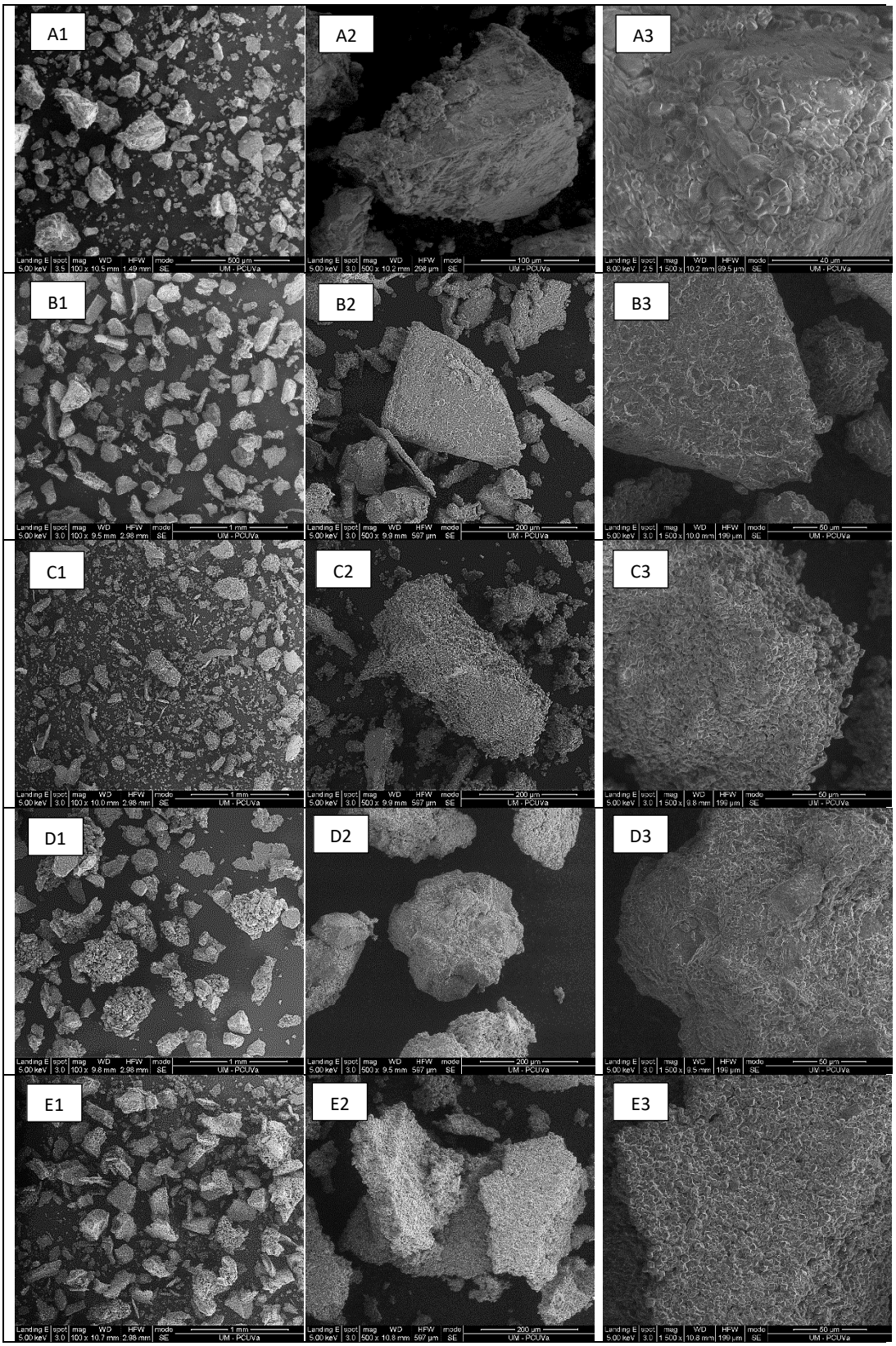

Figure 1. SEM images of the studied flours. (A) Control, (B) ANN-20, (C) US+ANN-20, (D) ANN-60 and (E) US+ANN-60 at a magnification of (1) 100x, (2) 500x and (3) 1500x.

Ultrasounds have been reported to cause general disruption of rice flour particles, generating smaller size particles (Vela et al., 2021). Particle size distribution was quantified to assess granulation and uniformity of studied flours (see Supplementary Fig. 1). In US+ANN samples, the appearance of a smaller size fraction (around 1 to 10 μm) was determined, while annealed samples showed the same profile presented by the control. Results showed to be significantly dependent on both temperature and ultrasonication, and on their interaction (temperature x ultrasonication). US+ANN-20 presented the most differences compared to control flour, confirming size reduction due to action of cavitation. Median diameter (D_{50}) values obtained were minimum at US+ANN-20 and US+ANN-40, being up to 79 % and 68 % lower than the control, while their size dispersions ((D_{90}-D_{10})/ D_{50}) were the highest (Table 2). Results also demonstrated that said small size fraction was clearly affected by higher temperatures, increasing D_{50} to 158 μm in US+ANN-60, which is even higher than control (146 μm). These results lead to the conclusion that destruction of small particles happens with treatments at higher temperatures, particularly temperatures closer to onset gelatinization temperature of native flour, possibly due to gelatinization of those smaller particles. Wang et al. (2017) determined that wheat starch suffered partial gelatinization and disruption of granules when annealed at 50°C, even if it was below its gelatinization temperature (55.6 °C). The 100x micrograph of US+ANN-60 (Fig 1.E1) also presented fewer proportion of small particles compared to those observed in US+ANN-20 (Fig 1.C1), despite being sonicated under the same conditions.

3.2 Effect of treatment on starch damage content

Damaged starch values of ANN and US+ANN samples are shown in Table 2. Damaged starch was dependent on temperature, ultrasonication and their double interaction. Values obtained for US+ANN samples increased with increasing temperature. Results indicated that sonication impacts significantly on starch structure, given that US+ANN starch damage values were significantly higher than control and their annealed counterpart, while within ANN samples only ANN-60 was significantly higher than control. Results for US+ANN-20 and US+ANN-40 indicated that flour particles disaggregation caused by cavitation does not generate important damage to the starch structure, which is more sensitive to be disrupted by high temperature. The highest increase was determined for US+ANN-60 followed by ANN-60, representing an increase of 145 % and 68 % with respect to native sample. This higher amount of damaged starch goes in agreement with results obtained in particle size distribution (section 3.1), supporting the idea that gelatinization of small particles happened in treatments carried at 60 °C.

3.3 Effect of treatment on hydration properties

WAC, WAI, WSI and SP are shown in Table 2. Temperature and ultrasonication, as well as their double interaction significantly affected ($p<0.001$) the hydration properties WAC was the property where sonicated flours showed fewer variation compared to control, and results showed that the modifications were mainly caused by ANN. This property refers to flour's capacity to associate with water, being influenced by hydrophilic parts in carbohydrates and proteins (Jitngarmkusol, Hongsuwankul, & Tananuwong, 2008). Since samples sonicated at low temperature (20 and 40 °C) were statistically equal to the control, it can be inferred that said binding sites were not particularly vulnerable to be increased by sonication. Higher WAC determined in US+ANN-50 and US+ANN-60 could be due to presence of more gelatinized starch, damaged starch and modified structure of proteins (Kumar, Sharma, & Singh, 2017). These results might be attributed to disrupted hydrogen bonds between amorphous and crystalline regions and slight expansion of the amorphous region, improving the hydrophilic tendency of starch molecules. WAI, WSI and SP were significantly modified by US+ANN, while ANN caused slight changes. Ultrasonication markedly increased WAI and SP, with values being up to 134 % and 132 % (US+ANN-20), respectively, higher than native flour, showing a decreasing trend with increasing temperature. The dramatic increase of these properties can be attributed to the disruptive effect of cavitation over flour particles, which leads to particle fragmentation and surface damage, increasing granules' exposed area, allowing higher water uptake and retention. Similar results have been reported in rice starch (Sujka & Jamroz, 2013) and rice flour (Vela et al., 2021). The combination of US with ANN had the opposite effect. Increasing temperature allowed mobility of amylose chains, propitiating amylose-amylose and amylose-amylopectin interactions. Said mobility led to crystalline structure rearrangement, which limits sample's interaction with water (Hoover & Vasanthan, 1994; Wang et al., 2017; Zavareze et al., 2011), leading to lower values among the US+ANN samples. The more packed structure after ANN made it harder for amorphous regions to hydrate, requiring higher temperature to achieve gelatinization, which restricted swelling capacity of annealed samples (Tester, Debon, & Sommerville, 2000). ANN also influenced a decrease of WAI and SP by destruction of smaller particles that came with increasing temperature, since small particles have wider relative surface area and can interact with water easier than bigger particles. WAI and SP values obtained at the highest treatment temperature (US+ANN-60) were still marked, being 73 % and 82 % respectively higher than control flour. In the case of WSI, moderate differences were found among treated samples and control. It can be inferred that both ANN and US led to a decrease of this parameter, except when combined at the highest studied temperature (US+ANN-60), representing twice the value determined for control. It has been pointed out by Zheng et al. (2013) that US destroy amylopectin chains,

increasing the amylose content in treated flours, which results in more compact gels, making it more difficult for the soluble compounds to overflow outside, leading to lower solubility values. WSI obtained for US+ANN-60, however, is thought to be derived from depolymerization caused by strong treatment conditions, increasing the content of soluble compounds. Higher WSI are positively related to damaged starch (Harasym, Satta, & Kaim, 2020), agreeing with the highest value obtained for US+ANN-60 (see section 3.2).

Table 2. Particle size distribution, content of damaged starch and hydration properties of the sonicated flours and the control (untreated/native) flour.

Sample	D_{50} (μm)	$(D_{90}-D_{10})/ D_{50}$	Starch damage (g/100g)	WAC (g/g)	WAI (g/g)	WSI (g/100g)	SP (g/g)
Control	146d	2.13b	6.9ab	1.13a	7.1ab	4.7c	7.4ab
ANN-20	113aB	2.26cA	6.5aA	1.09aA	7.4bcA	5.3cB	7.9cA
ANN-40	126bB	2.13bA	7.2bA	1.20bB	7.5cA	3.1bA	7.7bcA
ANN-50	134cB	1.97aA	6.8abA	1.23bA	7.0aA	3.2bA	7.2aA
ANN-60	139cA	2.06abA	11.6cA	1.45cB	8.4dA	2.3aA	8.6dA
SE	2	0.03	0.2	0.01	0.1	0.2	0.1
Control	146d	2.13b	6.9a	1.13ab	7.1a	4.7b	7.4a
US+ANN-20	30aA	4.40dB	7.8bB	1.09aA	16.6eB	3.4aA	17.2eB
US+ANN-40	47bA	5.09eB	8.4bB	1.12aA	15.9dB	3.5aA	16.5dB
US+ANN-50	112cA	2.75cB	9.6cB	1.18bA	15.0cB	4.4bB	15.7cB
US+ANN-60	158eB	2.04aA	16.9dB	1.25cA	12.3bB	9.4cB	13.5bB
SE	1	0.02	0.3	0.02	0.2	0.1	0.2
Analysis of variance and significance (p-values)							
(F1): Temp.	***	***	***	***	***	***	***
(F2): Sonication	***	***	***	***	***	***	***
(F1) x (F2)	***	***	***	***	***	***	***

D_{50}: median diameter; $(D_{90}-D_{10})/D_{50}$: size dispersion. WAC = Water absorption capacity. WAI = Water absorption index. WSI = Water solubility index. SP = Swelling power. Starch damage, WAC, WAI, WSI, SP are referred to dry matter.
SE: Pooled standard error from ANOVA. The different letters in the corresponding column within each studied factor indicate statistically significant differences between means at $p < 0.05$. Lowercase letters are used to compare the effect of the temperature and capital letters to compare the effect of the sonication.
Analysis of variance and significance: *** $p < 0.001$. ** $p < 0.01$. * $p < 0.05$. ns: not significant.

3.4 Effect of treatment on X-Ray diffraction (XRD) pattern

Figure 2 shows determined XRD patterns with their corresponding crystallinity content. Samples presented the characteristic A-type XRD pattern for cereals, with peaks in 15, 17, 18, 23 and 26°, as well as the reflection at 20°, generally associated to V-crystallinity (Villanueva, Harasym, et al., 2018). ANN samples showed patterns with similar intensity to the control. Chi et al. (2019) agree that

annealing does not alter XRD patterns of starches. US+ANN samples showed unchanged pattern shapes, however the calculated crystallinity content was slightly higher than their corresponding ANN sample and the control (see Fig. 2). It has been reported that ultrasonication causes small changes or no changes at all in starches and flours crystallinity content, depending on treatment conditions (Amini et al., 2015; Carmona-García et al., 2016; Kaur & Gill, 2019; Luo et al., 2008; Vela et al., 2021). The crystallinity calculated for ANN samples did not show a clear trend and were similar to the control. ANN-60 showed the lowest crystallinity value, which could be related to partial gelatinization. The effects of ANN on crystallinity depend on the type of starch, a slight reduced intercrystalline spacing may indicate that helical packing becomes more compact and organized (Zavareze et al., 2011). The increase obtained after US+ANN treatments seem to indicate a moderate reorganization within the starch granules. US mainly attack amylose chains (Luo et al., 2008) increasing the proportion of short-chained amylose chains, while ANN facilitates mobility of amorphous regions, allowing reorganization and resulting in more "glassy" (more rigid and less mobile) material (Tester & Debon, 2000; Zavareze et al., 2011). Said combined effect could lead to more stable configurations associated with a more packed structure and improved order of crystalline regions.

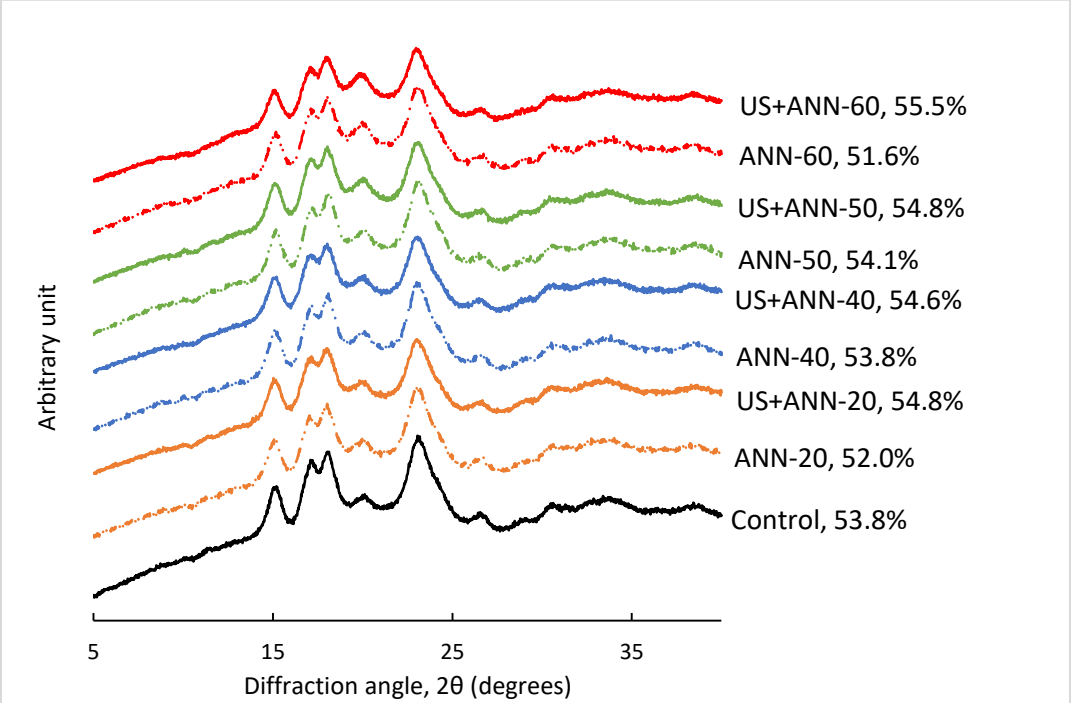

Figure 2. XRD pattern of control flour and flours treated at different temperatures. ANN treatments are represented by a discontinuous line and US+ANN treatments by a continuous line. The crystallinity degree of each sample is indicated on the curve.

3.5 Effect of treatment on FTIR spectra

Data used to evaluate changes on starch short-range/double helical order and on proteins secondary structure are presented in Table 3. Changes in carbohydrates are identified in the 1100-900 cm^{-1} region (see Supplementary Figure 2). Within this region, bands at 1047 cm^{-1} and 1022 cm^{-1} have been associated with starch crystalline and amorphous regions, respectively, while 995 cm^{-1} results from bonding in hydrated carbohydrate helices, particularly sensitive to water content in starch (due to C-OH bending vibrations) (Bajer, Kaczmarek, & Bajer, 2013; Monroy et al., 2018). The 1047/1022 ratio has been frequently used to quantify the degree of short-range order in starch, while the 1022/995 ratio is used to quantify the proportion of amorphous to ordered structure of starch (Yong et al., 2018). The 1047/1022 ratio of absorbance for ANN samples remained unchanged, with only ANN-60 being significantly different than control. This decrease was possibly related to low degree of partial gelatinization during treatment. Wang et al. (2017) also indicated that annealing did not modify the 1047/1022 ratio of starches. Sonicated samples presented reduced values of 1047/1022 ratio (0.659-0.672) compared to control (0.708), indicating disruption of short-range molecular order. Similar results have been reported in sonicated rice flour before (Vela et al., 2021). In the case of 1022/995 ratio, a significant increase was determined after sonication, referring to higher proportion of amorphous to ordered structure zones in the starch granules (Monroy et al., 2018). This indicates an increased proportion of short-chained amylose chains. The effect on these ratios does not seem to depend on treatment temperature.

Changes in the secondary structure of proteins were assessed in individual bands identified in the range of 1700-1600 cm^{-1} (see Supplementary Figure 3), corresponding to amide I, mainly due to C=O stretching vibration (~80 %) of the amide groups and some in-plane N-H bending (<20 %) (Kong & Yu, 2007). High sensitivity to small variations in molecular geometry and hydrogen bonding patterns makes amide I band particularly useful for analyzing changes in protein secondary structure (Kong & Yu, 2007). Relative area of each individual component was used to quantify changes provoked by treatments (Table 3). Results indicated that modifications on protein secondary structures were not dependent on temperature (with the exception of β-turn), but depended greatly on ultrasonication and their double interaction (Temperature x Ultrasonication). ANN led to high intensities around 1658 cm^{-1}, related with α–helix protein structures, similar to the control. It seems like α-helix structures were particularly affected by US at higher temperatures, given that in flours sonicated at 50 and 60 °C this value was reduced more than 80% with respect to control. β-sheet were significantly reduced by US+ANN, while ANN alone increased them. β-turn (4.3 % in control) were significantly increased by US+ANN (10 – 28 %), and remained unchanged after ANN. ANN reduced significantly the

random-coil structure regardless of the applied temperature. However, in ultrasonicated samples there was higher percentage attributed to random coil than the control, derived from the dissociative impact of cavitation. Determined changes are believed to be consequence of the shear forces of US mechanical action and the excess water used during treatments that enhanced the unfolding of protein molecule internal structure (Zavareze et al., 2011).

Table 3. Starch bands from FTIR analysis and secondary structure content of the studied samples.

	Starch bands		Protein secondary structure analysis (%)			
Sample	IR 1047/1022	IR 1022/995	α-Helix	β-Sheet	β-Turn	Random coil
Control	0.708b	0.845a	46.3ab	22.7a	4.3a	27c
ANN-20	0.706bB	0.876cA	45.2aB	35.5cB	4.7aA	15aA
ANN-40	0.706bB	0.864bA	46.0abB	31.2bB	4.8aA	18bA
ANN-50	0.706bB	0.860bA	49.9cB	29.6bB	4.6aA	16abA
ANN-60	0.679aB	0.845aA	47.7bcB	30.5bB	4.6aA	17abA
SE	0.002	0.003	0.7	0.6	0.2	1
Control	0.708c	0.845a	46d	22.7c	4a	27a
US+ANN-20	0.664abA	0.885bA	22cA	15.0aA	10aB	53cB
US+ANN-40	0.672bA	0.906bB	17bcA	17.9abA	19bB	47bB
US+ANN-50	0.659aA	0.894bB	7aA	17.4abA	28cB	48bB
US+ANN-60	0.666abA	0.887bB	9abA	18.9bA	23bcB	49bcB
SE	0.003	0.007	3	0.9	2	1
Analysis of variance and significance (p-values)						
(F1): Temp.	***	*	ns	ns	**	ns
(F2):Sonication	***	***	***	***	***	***
(F1) x (F2)	***	ns	**	***	**	*

SE: Pooled standard error from ANOVA. The different letters in the corresponding column within each studied factor indicate statistically significant differences between means at $p < 0.05$. Lowercase letters are used to compare the effect of the temperature and capital letters to compare the effect of the sonication.
Analysis of variance and significance: *** $p < 0.001$. ** $p < 0.01$. * $p < 0.05$. ns: not significant.

3.6 Effect of treatment on thermal properties

Thermal properties of phase transitions determined from gelatinization (first) and retrogradation (second) scans are shown in Table 4. Samples showed thermograms with two peaks, a bigger first one corresponding to starch gelatinization, and a smaller peak appearing at higher temperature due to amylose-lipid complex dissociation (Villanueva, Harasym, et al., 2018). Gelatinization enthalpy (ΔH_{gel}) was not significantly changed by ANN regardless of treatment temperature. However, the dual treatment (US+ANN) showed slight increase at 50 °C and significant reduction at 60 °C. Tester et al. (2000) stated that annealing enhances inter- and intra-helical interactions with little effect on enthalpy, which could explain why only slight, not significant, increases were determined, except at

50 ºC and 60 °C with the dual effect US+ANN. The lower value obtained for US+ANN-60 is thought to be consequence of partial gelatinization of small-size particles that was determined to occur during treatment (as determined in sections 3.1, 3.2 and 3.3). The effect US have on ΔH_{gel} is not uniform. Some authors indicated that after ultrasonication ΔH_{gel} increased due to rearrangement of the molecular packing within the granule microstructure (Carmona-García et al., 2016; Zhu & Li, 2019), while others found a reduction after US treatment (Amini et al., 2015; Jambrak et al., 2010; Luo et al., 2008). The modification depends greatly on treatment conditions (time and frequency) and sample's botanical origin (amylose/amylopectin composition). Gelatinization temperatures were not significantly modified by ANN alone, but the combination of US+ANN led to clear changes. Ultrasonication caused increase of $T_{O\text{-}gel}$ (at 50 and 60 °C) and significant decrease of $T_{E\text{-}get}$, which provokes narrowing of gelatinization temperature range (ΔT), while $T_{P\text{-}gel}$ was slightly increased. Said determined changes were greater the closer the treatment temperature was to $T_{O\text{-}gel}$ of native sample. US treatments, as well as ANN treatments, have been said to increase $T_{O\text{-}gel}$ and $T_{P\text{-}gel}$, decrease $T_{E\text{-}gel}$, and sharpen gelatinization temperature range ($\Delta T = T_{E\text{-}gel} - T_{O\text{-}gel}$) (Amini et al., 2015; Hoover & Vasanthan, 1994; Richard F. Tester & Debon, 2000). Based on results, it can be inferred that ultrasonication led to modification of said temperatures, and were potentiated when combining with ANN. Narrowing of ΔT was significantly influenced by both temperature and sonication, and their dual interaction ($p<0.001$). This may suggest that sonication distorted starch granules' amorphous and non-organized parts, increasing starch homogeneity due to a well-organized crystalline leftovers structure (Amini et al., 2015), whose mobility and greater order was enhanced by high temperature (Zavareze et al., 2011). Increase of $T_{O\text{-}gel}$ in US+ANN samples is thought to be caused by synergetic effect of both treatments. US mainly attack the amorphous regions in starch, increasing the proportion of short-chained amylose chains (Luo et al., 2008) while ANN improves the interaction among these chains, resulting in more susceptibility to the formation of double helices. The extent of the interaction is influenced by proximity of the treatment temperature to native sample's $T_{O\text{-}gel}$ (Hoover & Vasanthan, 1994). Significant decrease of $T_{E\text{-}gel}$ in sonicated samples is believed to be consequence of increased crystallinity order as a result of closer packing of the crystallites within the starch granule (Hoover & Vasanthan, 1994). These results go in agreement with the slight crystallinity increase obtained with X-ray diffraction data. Dissociation enthalpy of amylose-lipid inclusion complexes obtained for US+ANN samples in gelatinization scan (1.77-1.89 J/g) were significantly higher than control flour (1.37 J/g) and ANN counterparts (1.45-1.51 J/g). Onset temperatures of this peak ($T_{O\text{-}am\text{-}lip}$) were lower in sonicated samples. These results are thought to be consequence of higher availability of amylose chains in US+ANN samples due to disruption of the amorphous regions by ultrasonication (Amini et al., 2015; Vela et al., 2021).

Table 4. Thermal properties of treated flours and the control flour.

Sample	First scan							Second scan					
	ΔH_{gel} (J/g)	To_{-gel} (°C)	T_{P-gel} (°C)	T_{E-gel} (°C)	ΔT (°C)	ΔH_{am-lip} (J/g)	$T_{O-am-lip}$ (°C)	ΔH_{ret} (J/g)	To_{-ret} (°C)	T_{P-ret} (°C)	T_{E-ret} (°C)	ΔH_{am-lip} (J/g)	$T_{O-am-lip}$ (°C)
Control	9.6a	61.1a	74.6c	81.5a	20.4a	1.37a	89.4a	4.8a	36.6ab	51.4a	63.0bc	3.3a	88.2ab
ANN-20	9.2aA	61.0aA	73.9aA	81.2aB	20.2aB	1.48aA	89.2aA	4.9aB	36.8bA	51.2aA	63.4cA	3.2aA	89.4bB
ANN-40	9.5aA	61.2aA	74.4bcA	81.1aB	19.9aB	1.51aA	87.9aB	4.7aA	36.9bA	51.2aA	62.3aA	3.3aA	87.3aA
ANN-50	9.7aA	61.0aA	74.3bcA	80.9aB	19.6aB	1.45aA	88.7aB	4.6aB	36.9bA	51.1aA	62.7abA	3.4aA	87.6aA
ANN-60	9.5aB	61.0aA	74.1abA	81.1aB	20.1aB	1.47aA	89.3aB	4.7aA	36.2aA	51.5aA	62.8abA	3.5aA	87.6aB
SE	0.2	0.2	0.1	0.4	0.4	0.08	0.6	0.1	0.2	0.3	0.2	0.1	0.4
Control	9.6b	61.1a	74.6a	81.5b	20.4d	1.37a	89.4b	4.8c	36.6a	51.4a	63.0bc	3.3a	88.2b
US+ANN-20	9.5bA	61.7aB	74.4aB	79.5aA	17.8cA	1.77bB	88.0abA	4.0aA	37.6bA	50.7aA	62.7abA	3.3aA	88.1bA
US+ANN-40	9.7bA	61.3aA	74.3aA	79.3aA	18.0cA	1.85bB	86.1aA	4.4bA	37.6bA	50.6aA	62.5aA	3.3aA	88.1bA
US+ANN-50	10.2cB	62.9bB	74.6aA	79.7aA	16.8bA	1.87bB	86.1aA	4.3bA	36.6aA	51.0aA	62.4aA	3.1aA	87.9abA
US+ANN-60	8.6aA	68.7cB	75.1bB	79.4aA	10.8aA	1.89bB	87.4aA	4.8cA	37.4bB	51.4aA	63.1cB	3.2aA	86.7aA
SE	0.1	0.2	0.1	0.3	0.3	0.07	0.8	0.1	0.2	0.3	0.1	0.1	0.4
Analysis of variance and significance (p-values)													
(F1): Temp.	***	***	ns	ns	***	ns	ns	*	ns	ns	**	ns	**
(F2):Sonication	ns	***	*	***	***	***	**	***	**	ns	ns	ns	ns
(F1) x (F2)	***	***	**	ns	***	ns	ns	***	*	ns	*	ns	*

ΔH_{gel} = Enthalpy of gelatinisation. T_{O-gel}, T_{P-gel}, T_{E-gel}: Onset, peak and endset temperatures of gelatinization. $\Delta T = (T_{E-gel} - T_{O-gel})$. ΔH_{am-lip} = Enthalpy of the amylose-lipid dissociation. $T_{O-am-lip}$ = Onset temperature of the amylose-lipid complex dissociation. ΔH_{ret} = Enthalpy of melting of retrograded amylopectin. T_{O-ret}, T_{P-ret}, T_{E-ret}: Onset, peak and endset temperatures of melting of retrograded amylopectin. ΔH_{gel}, ΔH_{ret}, ΔH_{am-lip} are given in J/g dry matter.

SE: Pooled standard error from ANOVA. The different letters in the corresponding column within each studied factor indicate statistically significant differences between means at $p < 0.05$. Lowercase letters are used to compare the effect of the temperature and capital letters to compare the effect of the sonication.

Analysis of variance and significance: *** $p < 0.001$. ** $p < 0.01$. * $p < 0.05$. ns: not significant.

The second scan performed after 7 days of sample storage at 4 °C also led to two peaks; the main one associated to melting of recrystallized amylopectin, and a latter one corresponding to dissociation of amylose-lipid complex. The melting enthalpy of recrystallized amylopectin (ΔH_{ret}) of ANN samples did not show significant differences compared to control flour. However, in US-ANN samples, treatments performed at lower temperatures showed significantly lower values of ΔH_{ret}, indicating that this reduction may be generated by ultrasonication rather than annealing. Yu et al. (2013) reported decrease in ΔH_{ret} of rice starch after being ultrasonicated at 100 and 500 W. Even though US mainly attack amorphous regions, US can still destroy the branched molecule structure of amylopectin, leaving less recrystallized amylopectin in sonicated samples and finally decreasing the retrogradation enthalpy value (Yu et al., 2013). The enthalpy of the amylose-lipid complex was higher in the second scan, probably due to better conditions for complex formation after the first heating, because the leaking of amylose from granules that occurs at temperatures above gelatinization temperature range (Villanueva, Harasym, et al., 2018).

3.7 Effect of treatment on pasting properties

Pasting properties of studied flours are shown in Table 5. All pasting properties were significantly influenced by temperature, sonication and their double interaction. Pasting temperature (PT) denoted a delay in the beginning of gelatinisation of treated samples. Said delay supports the fact that annealing induces strengthening of intragranular bonded forces, resulting in starch requiring more heat before structural disintegration and paste formation occurs (Zavareze et al., 2011). US+ANN samples showed that US had a synergetic effect with ANN potentiating PT delay, following an increasing trend with increasing treatment temperature, getting to be up to 3.9 °C higher (US+ANN-50) than control. Ultrasonication led to general reduction of pasting profiles, being more prone with increasing temperature (Fig. 3). Pasting development in flours depends on their water-binding capacity, which results from combined starch, protein, and fiber water-binding capacities, susceptible to be modified by ultrasonication (Harasym et al., 2020). Similar behavior has been reported in quinoa (Zhu & Li, 2019), buckwheat (Harasym et al., 2020) and rice (Vela et al., 2021) flours, as well as maize (Luo et al., 2008), sweet potato (Zheng et al., 2013) and rice (Zuo et al., 2009) starches after sonication. The effect of ANN on pasting properties of flours and starches, on the contrary, is not as clear, leading to the conclusion that it mainly depends on treatment conditions and structural characteristic of the treated matter (Zavareze et al., 2011). Results seem to indicate that these profile reductions after sonication are potentiated with ANN, following a decreasing trend with increasing temperature.

Table 5. Pasting and rheological parameters of the studied flours.

Sample	PT (°C)	PV (Pa · s)	TV (Pa · s)	FV (Pa · s)	BV (Pa · s)	SV (Pa · s)	G_1' (Pa)	a	G_1'' (Pa)	b	$\tan(\delta)_1$	c	τ_{max} (Pa)	Cross over (Pa)
Control	80.3a	4.06c	1.77c	4.15d	2.37b	2.37c	187c	0.092a	31c	0.342a	0.165a	0.25a	121c	174b
ANN-20	81.4bA	3.82bB	1.70bcA	3.93cB	2.12aB	2.23bB	157bA	0.107abB	28bcB	0.344aA	0.172aB	0.24aA	85abA	141aA
ANN-40	81.5bA	3.61aB	1.53aA	3.65bA	2.08aB	2.13bB	152abA	0.105abB	27abcB	0.337aA	0.176abB	0.23aA	96bA	147aA
ANN-50	81.4bA	3.58aB	1.56aA	3.38aA	2.02aB	1.82aB	118aA	0.121bB	23aB	0.344aA	0.192bB	0.23aA	73aA	125aA
ANN-60	82.5cA	3.67aB	1.65abB	3.54bB	2.02aB	1.89aB	140abA	0.106abB	24abB	0.345aA	0.170aB	0.24aA	90bA	138aA
SE	0.3	0.04	0.05	0.05	0.07	0.06	12	0.008	2	0.005	0.007	0.01	6	9
Control	80.3a	4.06d	1.77b	4.15d	2.37d	2.37e	187c	0.092b	31c	0.342a	0.165b	0.25a	121b	174c
US+ANN-20	82.9bB	3.53cA	1.81bB	3.87cA	1.74cA	2.06dA	174bcA	0.078aA	20abA	0.367cB	0.123aA	0.29bB	147cB	174cB
US+ANN-40	83.1bB	3.53cA	1.81bB	3.66bA	1.75cA	1.85cA	159abA	0.087abA	22bA	0.358bcB	0.133aA	0.28bB	138cB	155bA
US+ANN-50	84.2cB	3.33bA	1.91cB	3.60bB	1.42bA	1.69bA	165bB	0.080abA	20abA	0.363bcB	0.126aA	0.28bB	107aB	151bB
US+ANN-60	83.9cB	2.38aA	1.49aA	2.86aA	0.88aA	1.36aA	141aA	0.083abA	19aA	0.355bB	0.137aA	0.27bB	101aA	123aA
SE	0.2	0.02	0.04	0.04	0.05	0.02	6	0.006	1	0.004	0.006	0.01	6	6
Analysis of variance and significance (p-values)														
(F1): Temp.	***	***	***	***	***	***	*	ns	*	*	*	ns	***	**
(F2):Sonication	***	***	***	***	***	***	**	***	***	***	***	***	***	*
(F1) x (F2)	**	***	***	***	***	***	ns	*	ns	ns	**	ns	***	**

PT = Pasting Temperature. PV = Peak Viscosity. TV = Trough Viscosity. FV = Final Viscosity. BV = Breakdown Viscosity. SV = Setback Viscosity. The power law model was fitted to frequency sweeps experimental data ($G' = G'_1 \cdot \omega^a$; $G'' = G''_1 \cdot \omega^b$; $\tan\delta = (\tan\delta)_1 \cdot \omega^c$) where G_1', G_1'' and $\tan(\delta)_1$ are the coefficients obtained from the fitting and represent the elastic and viscous moduli and loss tangent respectively, at a frequency of 1Hz. The *a*, *b* and *c* exponents quantify the dependence degree of dynamic moduli and the loss tangent with the oscillation frequency. τ_{max} represents the maximum stress tolerated by the sample in the LVR. SE: Pooled standard error from ANOVA. The different letters in the corresponding column within each studied factor indicate statistically significant differences between means at $p < 0.05$. Lowercase letters are used to compare the effect of the temperature and capital letters to compare the effect of the sonication. Analysis of variance and significance: *** $p < 0.001$. ** $p < 0.01$. * $p < 0.05$. ns: not significant.

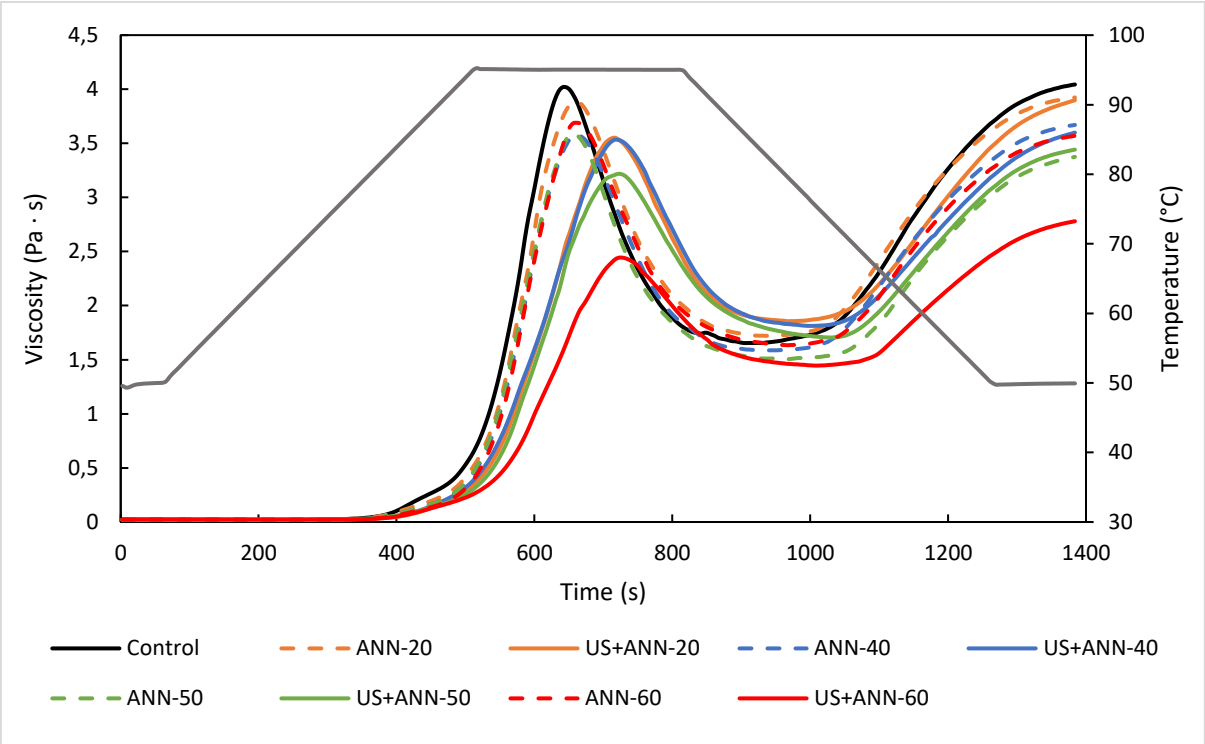

Figure 3. Pasting profile of control and treated flours. ANN treatments are represented by a discontinuous line and US+ANN treatments by a continuous line. The grey line corresponds to temperature (°C).

Previous studies agree on this behavior when combining sonication with high temperatures (Amini et al., 2015; Zuo et al., 2009). Peak viscosity (PV) reduction varied from 13 % (US+ANN-20) to 41 % (US+ANN-60). Amini et al. (2015) reported similar trend when sonicating corn starch at different temperatures, obtaining the most marked PV drop in sample sonicated at 65 °C. PV was achieved at a longer time in sonicated samples, graphically reflected as a profile displacement to the right (see Fig. 3). PT and PV results indicate reorganization within the starch molecule to thermodynamically more stable arrangement after US+ANN, requiring higher temperatures to hydrate amylose chains and longer exposure to 95 °C for water to completely hydrate the amorphous regions and fully gelatinize treated samples. The lowest PV value obtained for US+ANN-60 agrees with partial gelatinization observed in previous sections (sections 3.1, 3.2, 3.3 and 3.6), since the absence of the previously gelatinized particles limits the flour's pasting development capacity, in comparison to those samples sonicated at lower temperatures. Trough viscosity (TV) was significantly reduced by ANN, while, in general, a significant increase was determined for sonicated counterparts. US+ANN-60 was the only sonicated sample with TV significantly lower than the control, following the same trend showed by ANN. Final (FV), breakdown (BV) and setback (SV) viscosities also followed decreasing trend with increasing treatment temperature. Lower SV values indicate lower amylose

retrogradation. Few differences were shown by FV values between ANN and US+ANN at 20, 40 and 50 °C. However, at 60 °C a marked decrease was obtained after sonication. It indicates greater damaged caused to amylose chains resulting from synergetic effect of US and ANN at this temperature. BV was markedly reduced after sonication, with values being up to 63 % (US+ANN-60) lower than the control. This parameter gives information about stability of the samples, indicating their ability to withstand stress and heating. Significantly lower results can be related to internal granular structure rearrangement, as well as the structure of flour's proteins which by limiting starch swelling promote lower water absorption and lower viscosities.

3.8 Effect of treatment on the rheological properties of gels formed with the treated flours

Rheological properties of gels formed with the studied flours are shown in Table 5. All properties were found to be more significantly influenced by sonication than by temperature. Strain sweeps assays indicate two different regions in gels behavior, the linear viscoelastic region (LVR), where the elastic (G') and viscous (G") moduli as well as the loss tangent ($\tan(\delta) = G''/G'$) were constant, and the non-linear region, where gels quickly lose their structure's integrity, reaching the cross over point ($G' = G''$). The end of LVR is denoted by τ_{max}, which indicates the maximum value that gels are able to resist before disruption of their structure. Results showed significant increase of τ_{max} for US+ANN samples at 20 and 40 °C, and significant reduction at 50 and 60 °C, and progressive cross over decrease with increasing temperature. Cross over of all sonicated samples was found closer to τ_{max} than in control, indicating a quick collapse of gel structures after leaving the LVR. It is believed that the US effect in the combined treatment was the increase of τ_{max} given that at lower temperatures this value was increased in comparison to control, while the ANN effect seems to be the opposite, given that increasing treatment temperature led to a decrease of said parameter. A reduction of both τ_{max} and cross over was determined in all ANN samples, agreeing with this observed behavior. An increase of τ_{max} has been reported after sonication exposures as low as 10 min (Vela et al., 2021). Reduced values obtained with higher temperature are indicative of weaker gel structures with reduced resistance to breakage.

Frequency sweeps showed that G_1' exceeded G_1'' over the entire studied range, resulting in $\tan(\delta)_1$ values that classify their rheological behavior as "true" gels (Villanueva, Ronda, Moschakis, Lazaridou, & Biliaderis, 2018). Both ANN and US+ANN treatments led to similar reduction of G_1' with respect to control with slight differences among them. Only the 50 °C samples (ANN-50 and ANN+US-50) led to significantly different G_1' values (118 Pa versus 169 Pa). G_1'' showed significant differences between all studied temperature pairs, being lower in sonicated samples. Kaur & Gill

(2019) said that the decrease of G' and G" after sonication is caused by severe damaged over starch granules under shear forces induced by US, leading to straightening out of amylose molecules, reducing the shear action within the fluid layers and resulting in decreased viscosity. The linear amylose chains released during gelatinization were unable to form a consolidated compact network (Carmona-García et al., 2016). US+ANN led to lower $\tan(\delta)_1$ values than their ANN counterpart and control, indicative of higher solid-like behavior. This behavior could result from structural disorganization caused by US and the consequent association of polymeric chains to form the viscoelastic network (Monroy et al., 2018). No significant differences were found in $\tan(\delta)_1$ values among sonicated samples, indicating that change was not as dependent on treatment temperature, as it was on sonication time, since previous data has shown progressive reduction with increasing sonication time (Vela et al., 2021). It is believed that ultrasonication does not randomly break polymeric chains, since it is limited by a minimum chain length, once this limit is reached no further chain scission happens (Jambrak et al., 2010), which could explain these statistically equal results.

4. Conclusion

Treatment temperature was a determinative variable in the extent of modifications caused by US treatments on rice flour, modifying morphology, as well as functional, thermal, pasting and rheological properties. The closer the treatment temperature was to $T_{O\text{-}gel}$ of the native flour, the more marked the modification achieved. Cavitation effect led to general particle disruption and generation of smaller particles, causing a dramatic increase of WAI and SP, reaching values up to 134 % and 132 % (US+ANN-20) higher than control flour. The highest damaged starch and the lowest ΔH_{gel} obtained for US+ANN-60, as well as other evidence detected in particle size, pasting and rheological properties, reflect partial gelatinization at this treatment, even though 60 ºC was below control flour's onset gelatinization temperature. This behavior was not observed in ANN-60, which denotes synergistic effect of ANN and US treatments on flour physical modification. XRD and FTIR assays indicated changes caused to starch's long range and short range crystallinity, believed to be mainly due to increased proportion of short-chained amylose chains, and enhanced interaction among amylose chains and between amylose and outer branches of amylopectin due to mobility facilitated by annealing, leading to a thermodynamically more stable arrangement. Thermal properties agree on structural rearrangement after treatments, obtaining a decrease of $T_{O\text{-}gel}$ and $T_{P\text{-}gel}$, decrease of $T_{E\text{-}gel}$, and narrowing of ΔT, associated to closer packing of starch granule's crystallites. FTIR also showed significant modification of proteins secondary structure by both US and ANN, affecting all structures, indicating that proteins are prone to be modified by cavitation, leading to modifications of the flour's pasting and gel's rheological behavior, as they result from interaction among flour's components. US

decreased viscosity during pasting event, and caused a delay in the beginning of gelatinization and profile shift to the right, indicative of thermodynamically more stable arrangement. Ultrasonication led to formation of gels with higher strength, while higher treatment temperature led to weaker structures. Results prove that the effect of ultrasonication on the achieved flour modification can deeply vary depending on treatment temperature, so it is recommended to control the temperature during the whole treatment to avoid unwanted rises and sample degradation that could come from samples' gelatinization.

Acknowledgement

Authors thank the financial support of Ministerio de Economía y Competitividad and the European Regional Development Fund (FEDER) (AGL2015-63849-C2-2-R), the Ministerio de Ciencia e Innovación (PID2019-110809RB-I00) and the Junta de Castilla y León/FEDER VA195P20. A. Vela thanks the Junta de Castilla y León for the doctorate grant and M. Villanueva thanks the Alfonso Martín Escudero Foundation for the post-doctoral grant.

References

Abebe, W., Collar, C., & Ronda, F. (2015). Impact of variety type and particle size distribution on starch enzymatic hydrolysis and functional properties of tef flours. *Carbohydrate Polymers*, *115*, 260–268. https://doi.org/10.1016/j.carbpol.2014.08.080

Amini, A. M., Razavi, S. M. A., & Mortazavi, S. A. (2015). Morphological, physicochemical, and viscoelastic properties of sonicated corn starch. *Carbohydrate Polymers*, *122*, 282–292. https://doi.org/10.1016/j.carbpol.2015.01.020

Ashokkumar, M. (2015). Applications of ultrasound in food and bioprocessing. *Ultrasonics Sonochemistry*, *25*(1), 17–23. https://doi.org/10.1016/j.ultsonch.2014.08.012

Bajer, D., Kaczmarek, H., & Bajer, K. (2013). The structure and properties of different types of starch exposed to UV radiation : A comparative study. *Carbohydrate Polymers*, *98*, 477–482.

Byler, D. M., & Susi, H. (1986). Examination of the secondary structure of proteins by deconvolved FTIR spectra. *Biopolymers*, *25*(3), 469–487. https://doi.org/10.1002/bip.360250307

Carmona-García, R., Bello-Pérez, L. A., Aguirre-Cruz, A., Aparicio-Saguilán, A., Hernández-Torres, J., & Alvarez-Ramirez, J. (2016). Effect of ultrasonic treatment on the morphological, physicochemical, functional, and rheological properties of starches with different granule size. *Starch/Staerke*, *68*(9–10), 972–979. https://doi.org/10.1002/star.201600019

Chi, C., Li, X., Lu, P., Miao, S., Zhang, Y., & Chen, L. (2019). Dry heating and annealing treatment synergistically modulate starch structure and digestibility. *International Journal of Biological Macromolecules*, *137*(February 2020), 554–561. https://doi.org/10.1016/j.ijbiomac.2019.06.137

Harasym, J., Satta, E., & Kaim, U. (2020). Ultrasound treatment of buckwheat grains impacts important functional properties of resulting flour. *Molecules*, *25*(13), 1–15. https://doi.org/10.3390/molecules25133012

Hoover, R., & Vasanthan, T. (1994). The effect of annealing on the physicochemical properties of wheat, oat, potato and letil starches. *Journal of Food Biochemistry*, *17*, 303–325. https://doi.org/https://doi.org/10.1111/j.1745-4514.1993.tb00476.x

Jambrak, A. R., Herceg, Z., Šubarić, D., Babić, J., Brnčić, M., Brnčić, S. R., … Gelo, J. (2010). Ultrasound effect on physical properties of corn starch. *Carbohydrate Polymers*, *79*(1), 91–100. https://doi.org/10.1016/j.carbpol.2009.07.051

Jitngarmkusol, S., Hongsuwankul, J., & Tananuwong, K. (2008). Chemical compositions, functional properties, and microstructure of defatted macadamia flours. *Food Chemistry*, *110*(1), 23–30. https://doi.org/10.1016/j.foodchem.2008.01.050

Kaur, H., & Gill, B. S. (2019). Effect of high-intensity ultrasound treatment on nutritional, rheological and structural properties of starches obtained from different cereals. *International Journal of Biological Macromolecules*, *126*, 367–375. https://doi.org/10.1016/j.ijbiomac.2018.12.149

Kong, J., & Yu, S. (2007). Fourier Transform Infrared Spectroscopic Analysis of Protein Secondary Structures Protein FTIR Data Analysis and Band Assign-. *Acta Biochimica et Biophysica Sinica*, *39*(20745001), 549–559. https://doi.org/10.1111/j.1745-7270.2007.00320.x

Kumar, V., Sharma, H. K., & Singh, K. (2017). Effect of precooking on drying kinetics of taro (Colocasia esculenta) slices and quality of its flours. *Food Bioscience*, *20*(August), 178–186. https://doi.org/10.1016/j.fbio.2017.10.003

Luo, Z., Fu, X., He, X., Luo, F., Gao, Q., & Yu, S. (2008). Effect of ultrasonic treatment on the physicochemical properties of maize starches differing in amylose content. *Starch/Staerke*, *60*(11), 646–653. https://doi.org/10.1002/star.200800014

Monroy, Y., Rivero, S., & García, M. A. (2018). Microstructural and techno-functional properties

of cassava starch modified by ultrasound. *Ultrasonics - Sonochemistry*, *42*(November 2017), 795–804. https://doi.org/10.1016/j.ultsonch.2017.12.048

Ronda, F., Villanueva, M., & Collar, C. (2014). Influence of acidification on dough viscoelasticity of gluten-free rice starch-based dough matrices enriched with exogenous protein. *LWT - Food Science and Technology*, *59*(1), 12–20. https://doi.org/10.1016/j.lwt.2014.05.052

Sujka, M., & Jamroz, J. (2013). Ultrasound-treated starch: SEM and TEM imaging, and functional behaviour. *Food Hydrocolloids*, *31*(2), 413–419. https://doi.org/10.1016/j.foodhyd.2012.11.027

Tester, R F, Debon, S. J. J., & Sommerville, M. D. (2000). Annealing of maize starch, *42*, 287–299. https://doi.org/https://doi.org/10.1016/S0144-8617(99)00170-8

Tester, R. F., & Debon, S. J. J. (2000). Annealing of starch — a review. *International Journal of Biological Macromolecules*, *27*, 1–12. https://doi.org/https://doi.org/10.1016/S0141-8130(99)00121-X

Vela, A. J., Villanueva, M., Solaesa, Á. G., & Ronda, F. (2021). Impact of high-intensity ultrasound waves on structural, functional, thermal and rheological properties of rice flour and its biopolymers structural features. *Food Hydrocolloids*, *113*, 106480. https://doi.org/10.1016/j.foodhyd.2020.106480

Villanueva, M., Harasym, J., Muñoz, J. M., & Ronda, F. (2018). Microwave absorption capacity of rice flour. Impact of the radiation on rice flour microstructure, thermal and viscometric properties. *Journal of Food Engineering*, *224*, 156–164. https://doi.org/10.1016/j.jfoodeng.2017.12.030

Villanueva, M., Ronda, F., Moschakis, T., Lazaridou, A., & Biliaderis, C. G. (2018). Impact of acidification and protein fortification on thermal properties of rice, potato and tapioca starches and rheological behaviour of their gels. *Food Hydrocolloids*, *79*, 20–29. https://doi.org/10.1016/j.foodhyd.2017.12.022

Wang, S., Wang, J., Wang, S., & Wang, S. (2017). Annealing improves paste viscosity and stability of starch. *Food Hydrocolloids*, *62*, 203–211. https://doi.org/10.1016/j.foodhyd.2016.08.006

Witczak, M., Ziobro, R., Juszczak, L., & Korus, J. (2016). Starch and starch derivatives in gluten-free systems – A review. *Journal of Cereal Science*, *67*, 46–57. https://doi.org/https://doi.org/10.1016/j.jcs.2015.07.007

Yong, H., Wang, X., Sun, J., Fang, Y., Liu, J., & Jin, C. (2018). Comparison of the structural characterization and physicochemical properties of starches from seven purple sweet potato varieties cultivated in China. *International Journal of Biological Macromolecules*, *120*(1), 1632–1638. https://doi.org/10.1016/j.ijbiomac.2018.09.182

Yu, S., Zhang, Y., Ge, Y., Zhang, Y., Sun, T., Jiao, Y., & Zheng, X. Q. (2013). Effects of ultrasound processing on the thermal and retrogradation properties of nonwaxy rice starch. *Journal of Food Process Engineering*, *36*(6), 793–802. https://doi.org/10.1111/jfpe.12048

Zavareze, R., Renato, A., & Dias, G. (2011). Impact of heat-moisture treatment and annealing in starches : A review. *Carbohydrate Polymers*, *83*(2), 317–328. https://doi.org/10.1016/j.carbpol.2010.08.064

Zheng, J., Li, Q., Hu, A., Yang, L., Lu, J., Zhang, X., & Lin, Q. (2013). Dual-frequency ultrasound effect on structure and properties of sweet potato starch. *Starch/Staerke*, *65*(7–8), 621–627. https://doi.org/10.1002/star.201200197

Zhu, F. (2015). Impact of ultrasound on structure, physicochemical properties, modifications, and applications of starch. *Trends in Food Science and Technology*, *43*(1), 1–17. https://doi.org/10.1016/j.tifs.2014.12.008

Zhu, F., & Li, H. (2019). Modification of quinoa flour functionality using ultrasound. *Ultrasonics Sonochemistry*, *52*(November), 305–310. https://doi.org/10.1016/j.ultsonch.2018.11.027

Zuo, J. Y., Knoerzer, K., Mawson, R., Kentish, S., & Ashokkumar, M. (2009). The pasting properties of sonicated waxy rice starch suspensions. *Ultrasonics Sonochemistry*, *16*(4), 462–468. https://doi.org/10.1016/j.ultsonch.2009.01.002

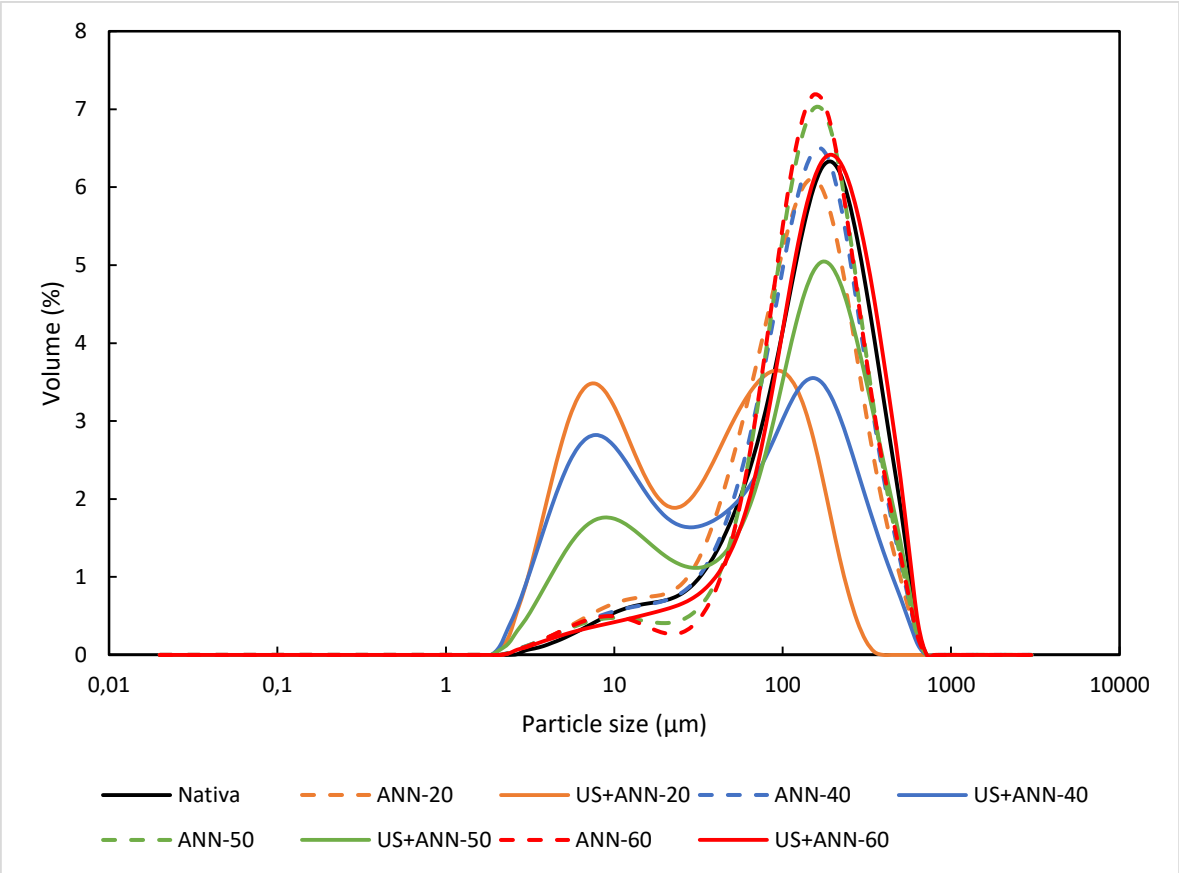

Supplementary Figure 1. Particle size distribution of the studied flours. ANN treatments are represented by a discontinuous line and US+ANN treatments by a continuous line.

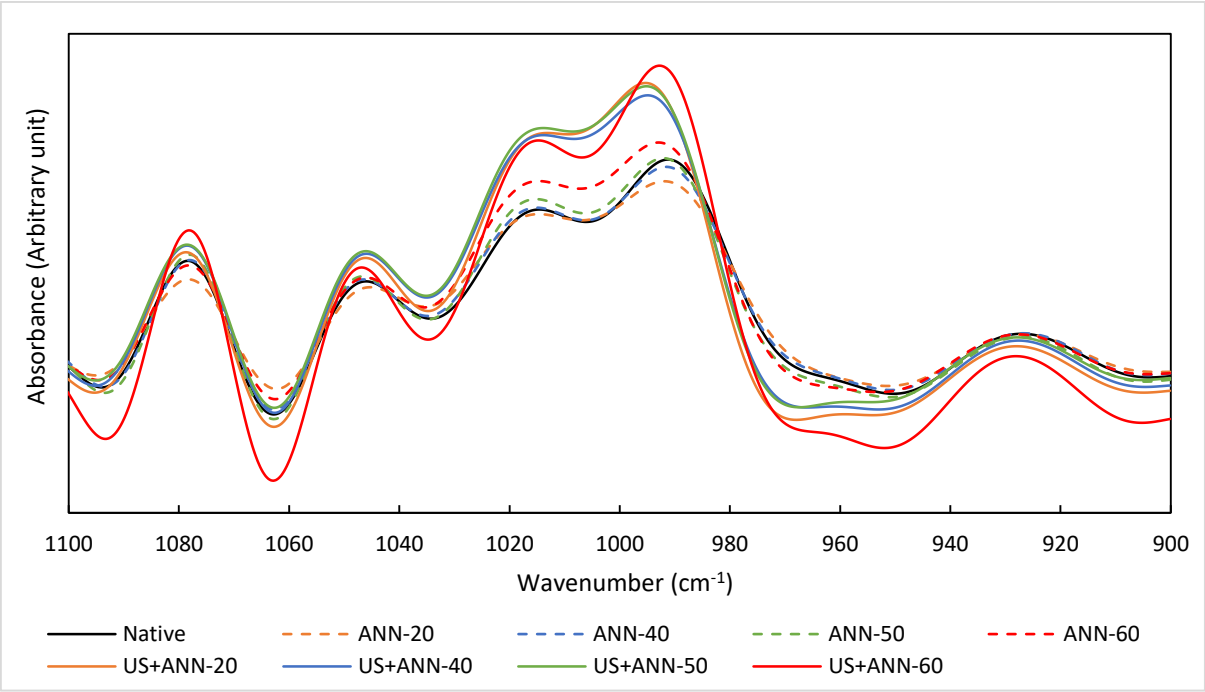

Supplementary Figure 2. FTIR spectra of studied samples in the region used to assess starch structural changes.

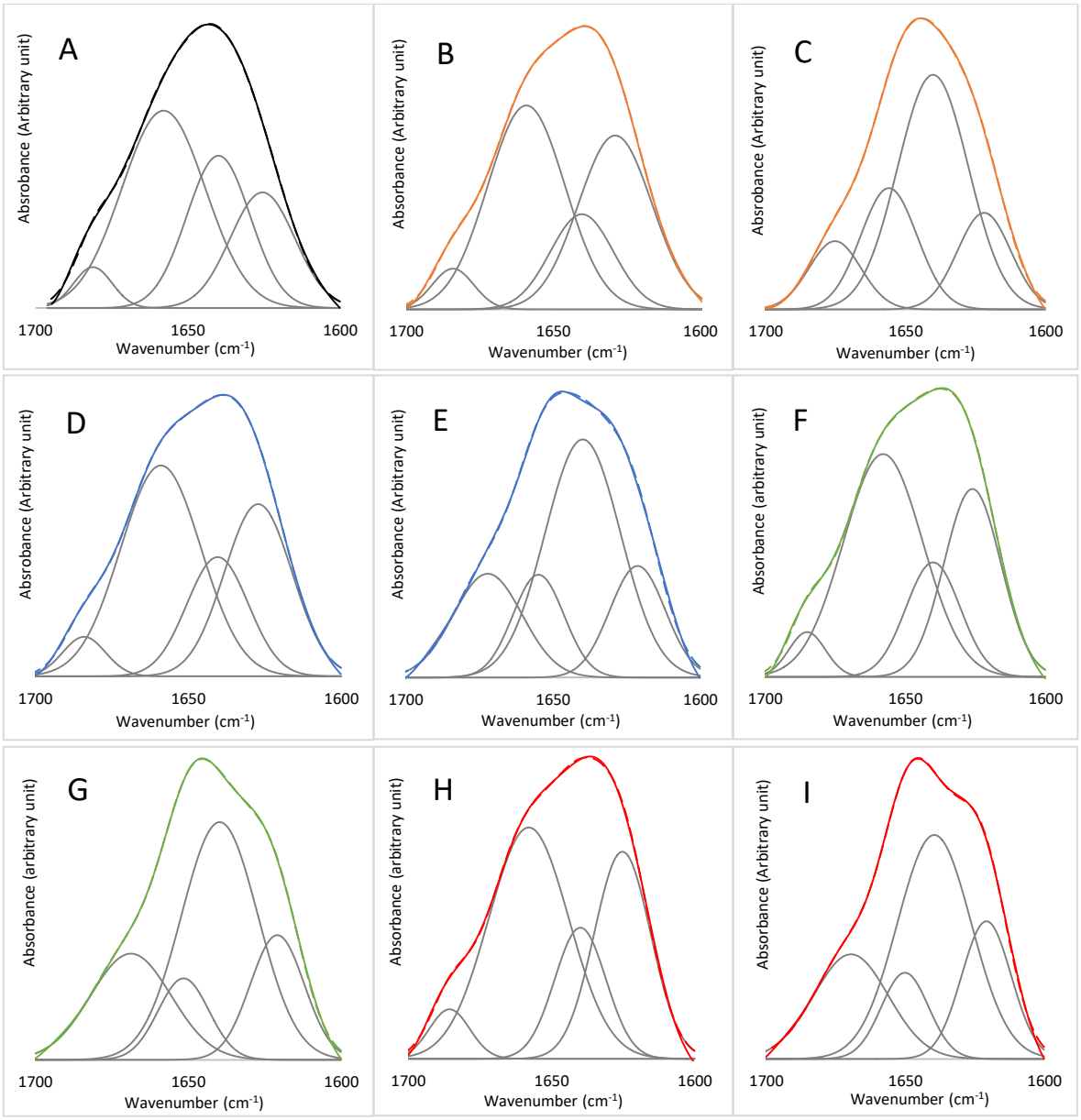

Supplementary Figure 3. Deconvolved amide I bands of the studied flours. A) Control; B) ANN-20; C) US+ANN-20; D) ANN-40; E) US+ANN-40; F) ANN-50; G) US+ANN-50; H) ANN-60; I) US+ANN-60. The continuous and discontinuous lines represent the deconvolved FTIR spectra and the fitted curve, respectively. Bands: β-turns (1700-1660 cm^{-1}), α-helix (1658-1650 cm^{-1}), random coil (1650-1640 cm^{-1}) and β-sheet (1640-1600 cm^{-1}).